Proc. Indian Acad. Sci. (Earth Planet. Sci.), Vol. 100, No. 1, March 1991, pp. 55–68.

Premonsoonal water characteristics and circulation in the east central Arabian Sea

V RAMESH BABU, J S SASTRY, V V GOPALAKRISHNA and D V RAMA RAJU

National Institute of Oceanography, Dona Paula, Goa 403 004, India

MS received 19 January 1990; revised 15 September 1990

Abstract. The hydrographic structure in the east central Arabian Sea during premonsoon period undergoes significant temporal change in the thermal field of upper 100 m, wherein temperature rises by about 0·5°C on an average from May to June. The major contribution in increasing the surface layer temperature comes from surface heat exchange processes, while the horizontal advective process tends to remove the heat from the upper layer. The geostrophic flow patterns are similar from May to June in the major part of the study area while in the coastal areas off Goa a southerly current sets in June in response to coastal upwelling.

Keywords. Water characteristics; circulation; premonsoon; east central Arabian Sea.

1. Introduction

Changes in circulation, especially in the upper layer of the north Indian Ocean take place due to the semi-annual reversal of winds. The International Monsoon Experiment (MONEX) was mainly concerned with the evolution of the Arabian Sea cooling, and the flow field in relation to the summer monsoon of 1979 (Krishnamurti 1981; Leetmaa *et al* 1982; Swallow *et al* 1983; Ramesh Babu and Sastry 1984; Rao 1984). However, the premonsoonal modifications in the hydrographic structure of the Arabian Sea particularly in its eastern region, have not been studied. The National Institute of Oceanography (NIO) was actively involved in the summer MONEX 1979 field programme by collecting oceanographic data along selected sections in the east central Arabian Sea in May and June. This paper reports the results of a study on the temporal and spatial variabilities in hydrographic characteristics, and the circulation in the east central Arabian Sea prior to the onset of the summer monsoon.

2. Data and method

The Indian Research Vessel R V Gaveshani had surveyed the east central Arabian Sea during May–June 1979 as a part of MONEX. During the first phase, the ship occupied oceanographic stations from 21 May to 3 June and the observations, except a few along 15°N, were repeated from 8 to 17 June in the second phase. Figure 1 shows the area of study along with station locations. Observations were not completed along 15°N due to heavy seas associated with an onset vortex (Krishnamurti *et al* 1979) which passed across the area during 15–17 June. In view of the delayed onset of

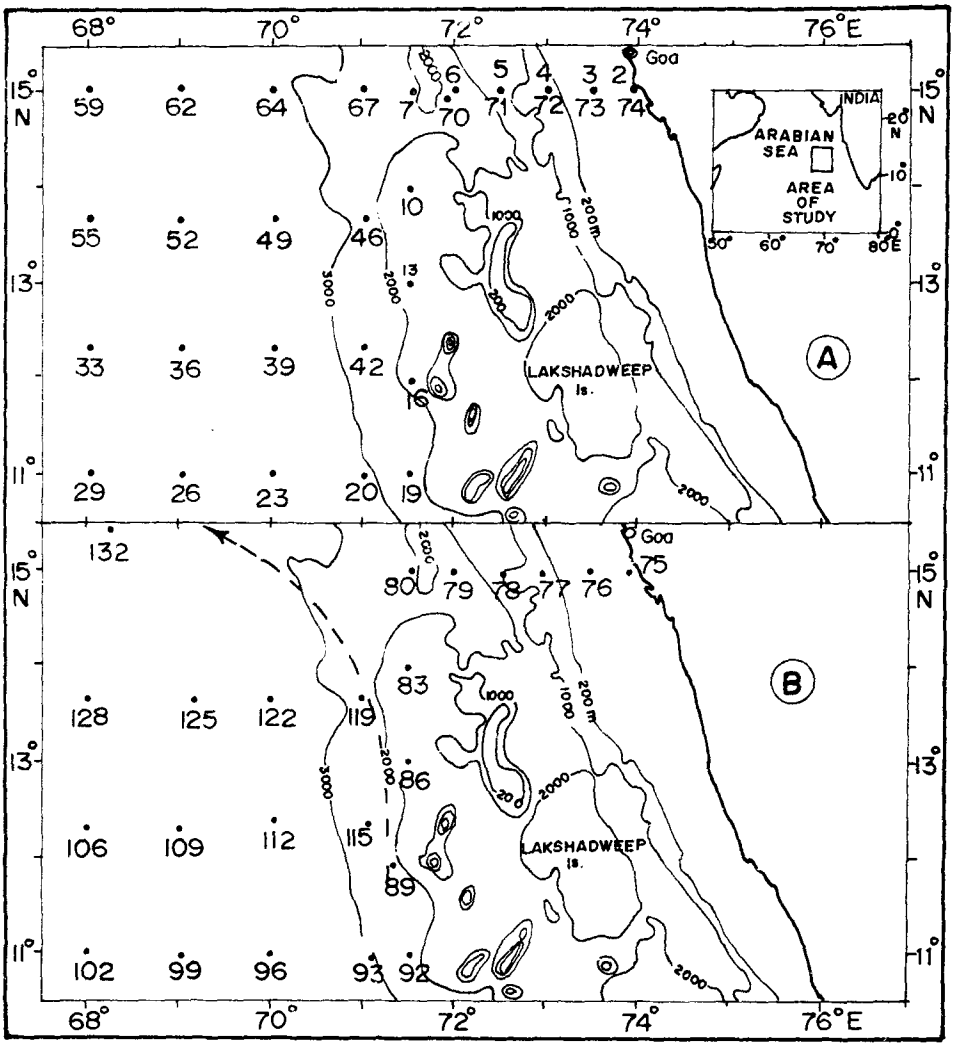

Figure 1. Station locations (dots) during (A) first phase (21 May to 3 June) and (B) second phase (8 to 17 June). The numbers below the dots represent those of the oceanographic stations. Full lines are depth contours. The track of an onset atmospheric vortex during second phase is shown as dashed line.

monsoon in 1979, the second phase, which was strictly not a premonsoon period and initially intended for studying hydrographical features immediately after the onset, now represents the conditions immediately preceeding the monsoon in early June. Thus, variations in the structure of the water column may be considered as progressive temporal changes.

The hydrographic data up to 1500 m were obtained by standard techniques. Salinities of water samples were estimated using a shipborne salinometer (model "Autosal" with an accuracy: $\pm$ 0·003‰). The vertical, as well as the horizontal distribution of temperature, salinity and density was constructed by deriving the necessary information from T–S curves, which were drawn for each station. The data

of the analysed fields have temperature, salinity and depth accuracies of ± 0·05°C, ± 0·01‰ and ± 5 m respectively. The geostrophic circulation at different horizontal levels was derived through routine dynamic calculations. The relative values of velocity were transferred into absolute ones by using a reference layer of zero motion, wherein the isobaric surfaces coincide with level surfaces. Following Bennet (1970), the reference depth was assumed to be at 1000 m, even though different depths were adopted for the Arabian Sea by other investigators (Zakilinskii 1964; Swallow and Bruce 1966; Bruce 1968; Sundara Raman and Murthy 1968; Varadachari *et al* 1968; Sastry and D'Souza 1972; Sharma 1976). For shallow regions, the dynamic computations were extended following the classical Hallend Hansen method (Sverdrup *et al* 1942).

3. Results

Figure 2 shows the average May and June temperature and salinity depth profiles in the 1500 m water column of the study area. It was clear that the water mass, except in the upper 100 m did not undergo significant temporal variations from phase I (May) to phase II (June). Hence, the description of the results of this study is limited to the upper 100 m.

3.1 *Thermal structure*

During the second phase, the sea surface temperature (SST) on an average was higher than what prevailed during the first phase (figures 3a–i and ii). Further, the SST decreased towards the Indian coast in both phases. The temperature at 50 m remained around 28·5 C during both phases, except for a temporal rise in the coastal region off Goa. Relatively cold waters (28°C) were also encountered in the northwestern

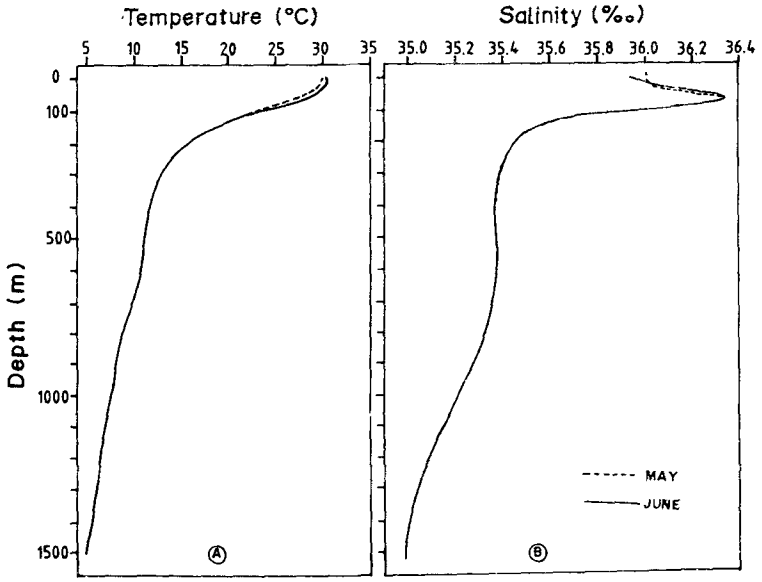

Figure 2. Average depth profiles of temperature (A) and salinity (B) for May and June 1979.

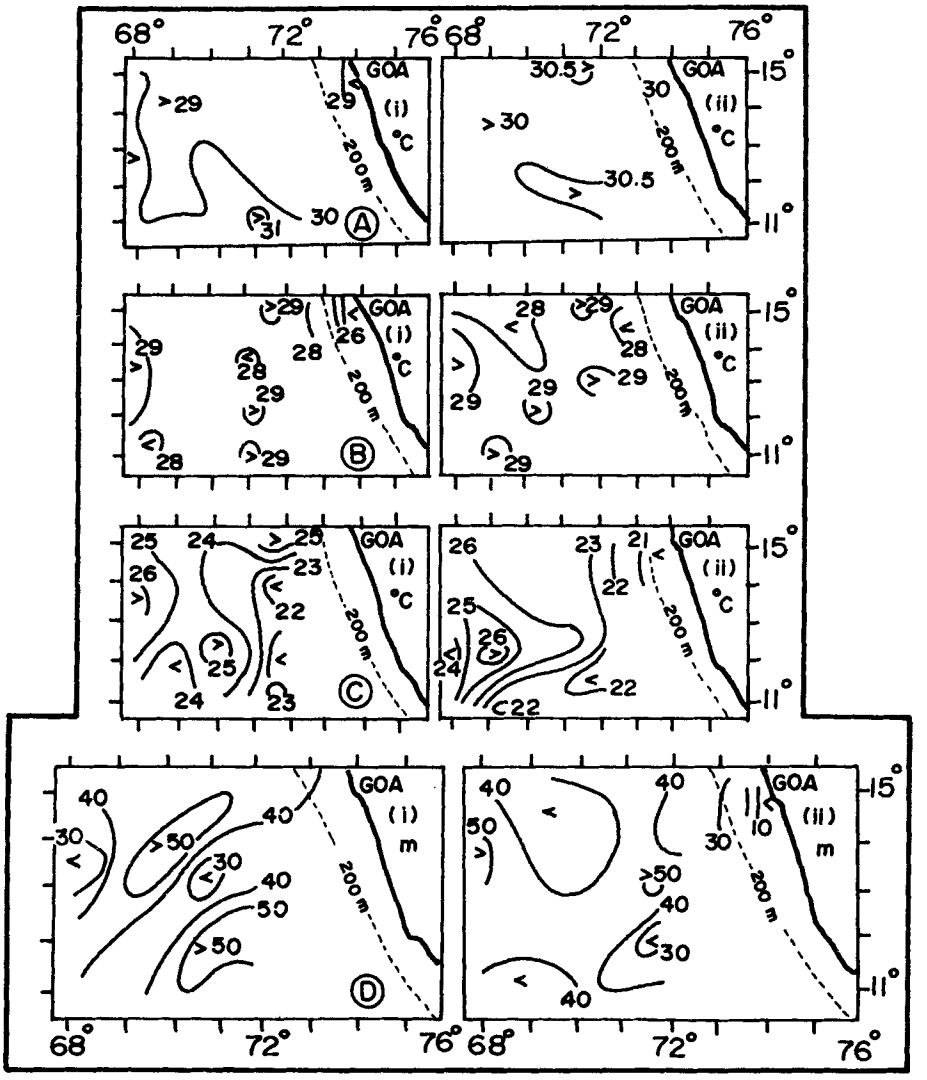

Figure 3. Temperature at (A) 0 m, (B) 50 m, (C) 100 m and (D) Depth of thermocline during first (i) and second (ii) phases.

region during the second phase (figure 3b–ii). This low temperature area was associated with a decrease in the mixed layer thickness (defined as the depth at which the temperature is less by 1°C to that at the surface) by about 10 m from May to June (figures 3d–i and ii). The east-west temperature gradient, with the incidence of lower temperatures towards the Indian coast become more prominent at 100 m—a feature that was seen in both phases (figure 3c). The thickness of the surface layer varied between 30 and 50 m during May and June (figure 3d). In general, it was lower during the second phase, and its presence at very shallow depths (10 m) in the nearshore regions off Goa was a conspicuous feature of the second phase.

3.2 *Upwelling off Goa*

A zonal section along 15°N across the self off Goa was covered thrice during the observational period (figure 4). The thermal structure in the upper thermocline, in general, showed an upslope of isotherms towards the west coast of India. During the third week of May (figure 4a–i), a shallow isothermal layer (30 m) was seen near the coast (Stn 2). After about 10 days, the thermocline rose to the surface at the same location (Stn 74), where it remained during the later part of the study period. The variability of thermal structure in the upper 100 m water column suggests that coastal upwelling might already be taking place and by June, the upwelled waters reached

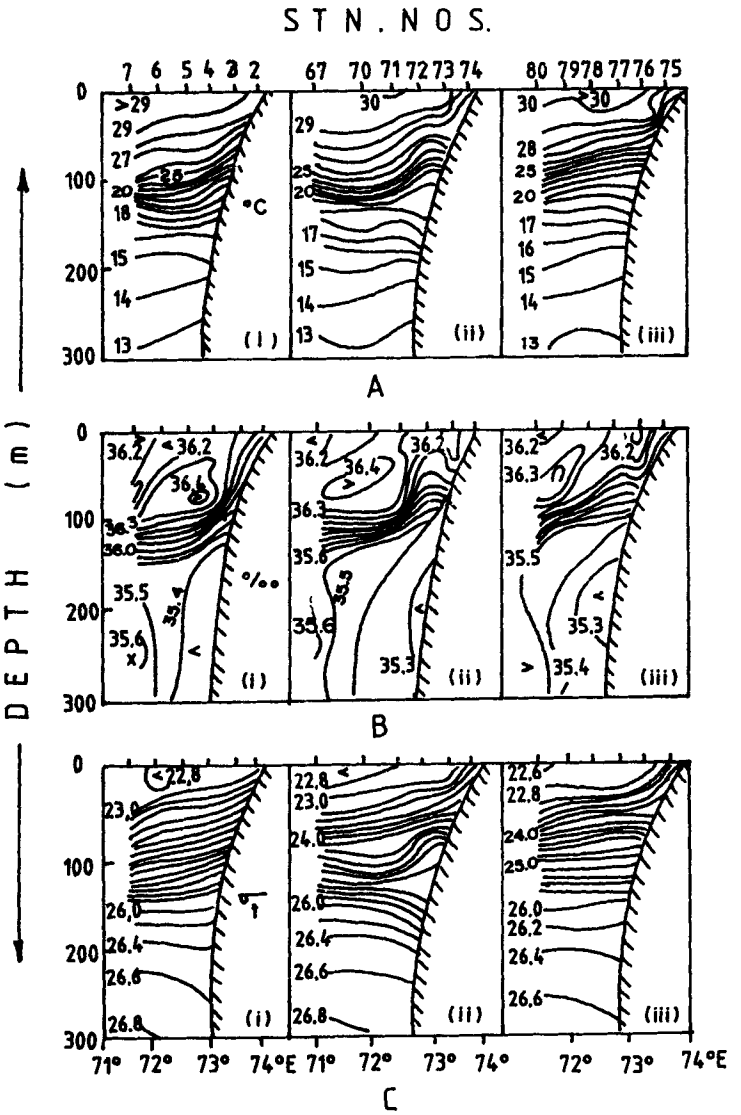

Figure 4. (A) Temperature (B) Salinity and (C) σ_t off Goa during (i) 21–23 May, (ii) 2–3 June and (iii) 8–9 June.

the surface in the nearshore regions off Goa. This is in agreement with the picture reported earlier by Sharma (1968a, b). The salinity field in association with upwelling is not variable with the result that the coastal upwelled waters have higher density (figures 4b and c).

3.3 *Salinity and water masses*

The surface salinity increased from southeast to northwest in the study area (figure 5a). But it decreased in the northwest by about 0·2‰ and increased by about the same magnitude in the southeast from May to June. Similar changes were also noticed at 50 and 100 m depths (figures 5b and c) thereby maintaining an uniform average salinity in the upper 100 m.

A sub-surface salinity maximum in the upper layers (> 36·3‰) as shown in figures 4b and 6b could be attributed to the spreading of the Arabian Sea high salinity water mass, which forms over most of the northern and eastern Arabian Sea. This is an outcome of excessive annual evaporation over precipitation. The core layer depth decreases towards the east, especially in the northern area of study (figures 4b and

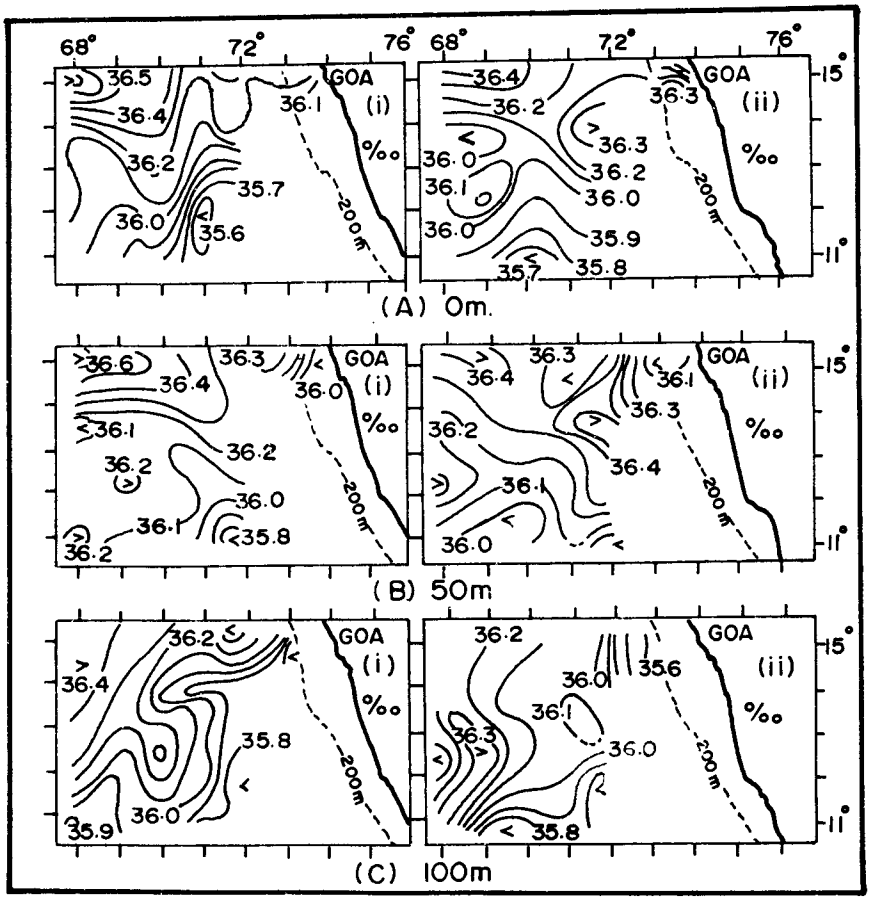

Figure 5. Salinity at (A) 0 m, (B) 50 m and (C) 100 m during the first (i) and second (ii) phases.

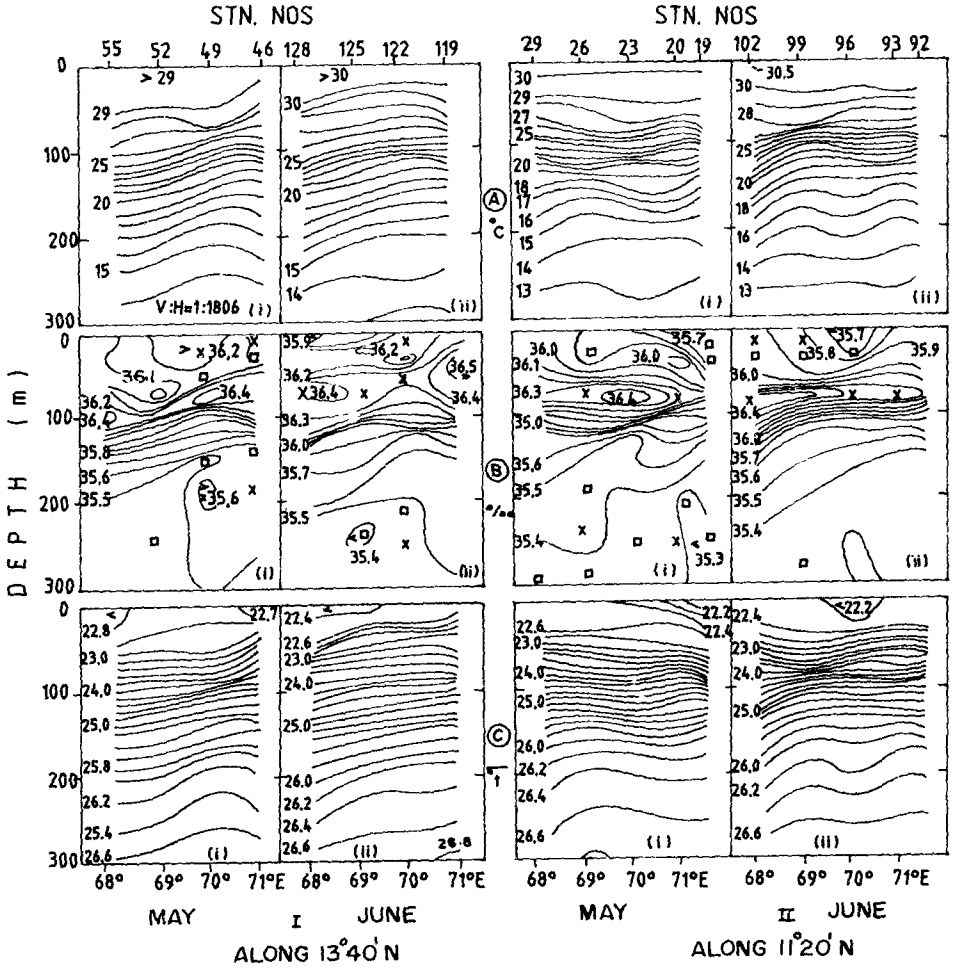

Figure 6. (A) Temperature (B) salinity and (C) σ_t along 13° 40′N (I) and 11°N (II) during the first (i) and second (ii) phases.

6b–I) while in the lower latitudes, the zonal upslope of the core layer is not prominent (figure 6b–II). However, the core of the Arabian sea high salinity water mass, observed near the surface at Stns 59 and 132 in the northwestern part of the area (figure 7b–I) loses its salinity by about 0·2‰ from May to June, but gains salinity in the eastern part at stations 10 and 13 by the same magnitude (figure 7b–II). A comparison of the vertical salinity distributions in the two phases indicates that the salinity in Arabian sea high salinity water mass increases slightly (figures 6b and 7b).

3.4 *Density* [σ_t] *and geostrophic circulation*

The density (σ_t) fields at the surface and at 50 m were influenced by salinity distribution (figures 8a, b and 5a, b). At 100 m, an eastward increase in σ_t was due to the corresponding decrease in temperature (figures 8c and 3c) which had resulted in a southerly flow in the upper layers of the western part of the study area during May (figure 9a, b, c–i). The flow pattern for June (figures 9a, b, c–ii) was more or less similar

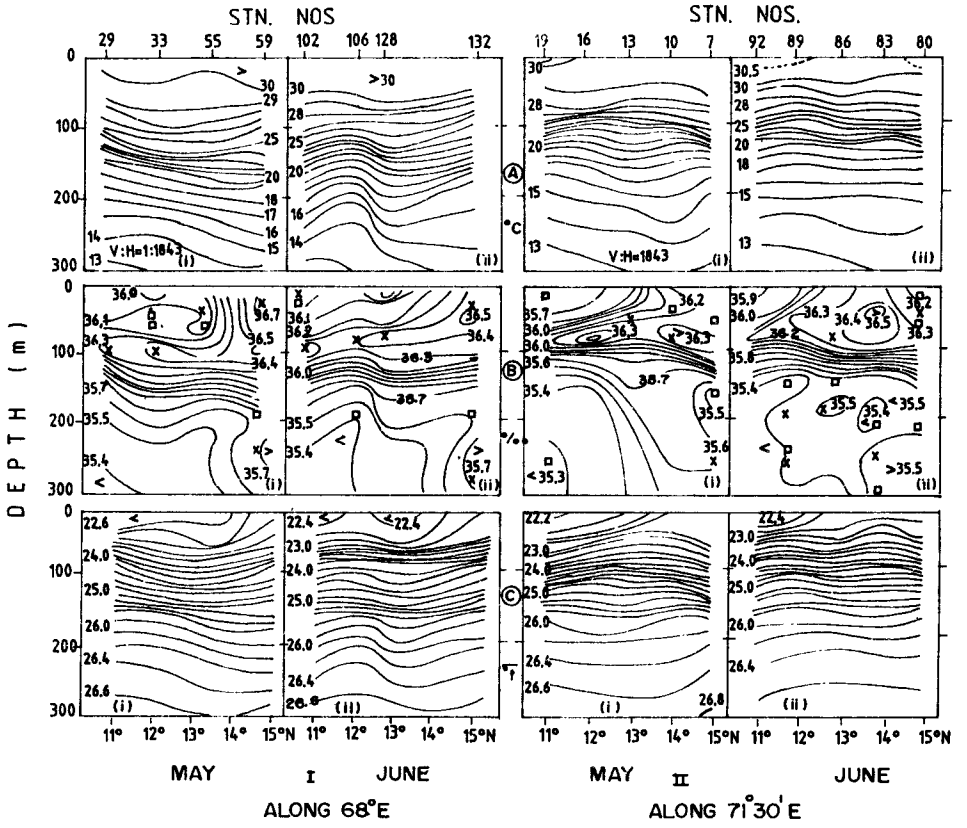

Figure 7. (A) Temperature, (B) salinity and (C) σ_t along 68°E (I) and 71° 30'E (II) during the first (i) and second (ii) phases.

to that in May, except along 70°E between 13°N and 15°N, where the current was directed towards southeast. Further, in June a cyclonic gyre near Lakshadweep Islands (12°N, 71·5°E) was found to be developing on account of a decrease in the depth of thermocline (figure 3). Off Goa coast, a southerly surface current was set in response to coastal upwelling during June. In general, the surface currents were of the order of 0·4 ms^{-1} during both phases.

4. Discussion

To distinguish the changes more clearly for the upper 100 m water column, the average T–S structures for May and June phases were constructed. They are shown in figure 10. On an average, the layer temperature rises by about 0·5°C in the upper water column while the salinity change was not significant. This led to a decrease of density in the surface layer. The increase in surface layer temperature was obtained after averaging the data over the area of study. Though the coastal region off Goa was marked by a decrease in surface layer temperature from May to June, this was offset by warming over a large part of the study area.

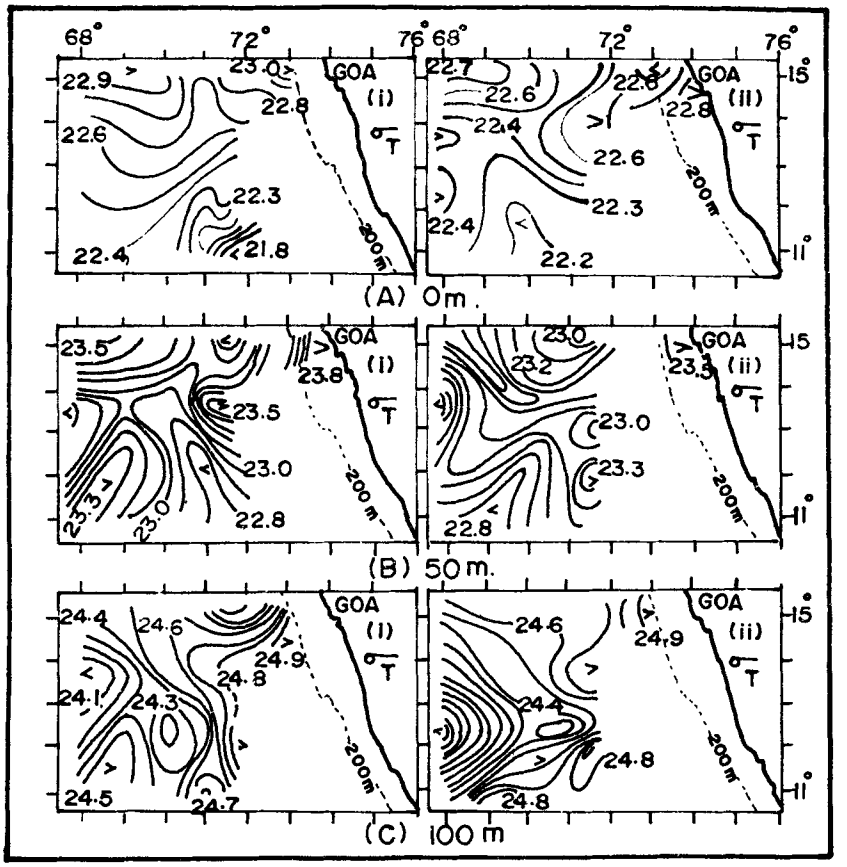

Figure 8. σ_t at (A) 0 m, (B) 50 m and (C) 100 m during the first (i) and second (ii) phases.

The increase in the surface layer temperature from May to June was examined by the following expression for the heat budget:

$$\frac{\partial H}{\partial t} = -\left(u\frac{\partial H}{\partial x} + v\frac{\partial H}{\partial y}\right) + R, \tag{1}$$

where u, v are the velocity components along x and y axes directed positive towards the east and west respectively; H is the heat content of the water column in the upper 100 m and R is the net surface heat exchange. This equation was considered after assuming negligible vertical advection and eddy diffusion in the open oceanic regions away from the boundary areas of coastal upwelling. The contributions of surface exchange and advective processes were specified for the upper 100 m water column. For computing the geostrophic transport and associated advective heat flux, a region (11° 00′ to 13° 40′N; 68° 00′ to 71° 00′E) with 1·0° lat × 1·3° long resolution, where observation were taken uniformly in both phases, was selected. Table 1a gives the average surface meteorological observations in the sub-area separately for the two phases. A substantial increase in cloudiness was seen from May to June, indicating the development of premonsoonal thunderstorms over the area. The surface heat

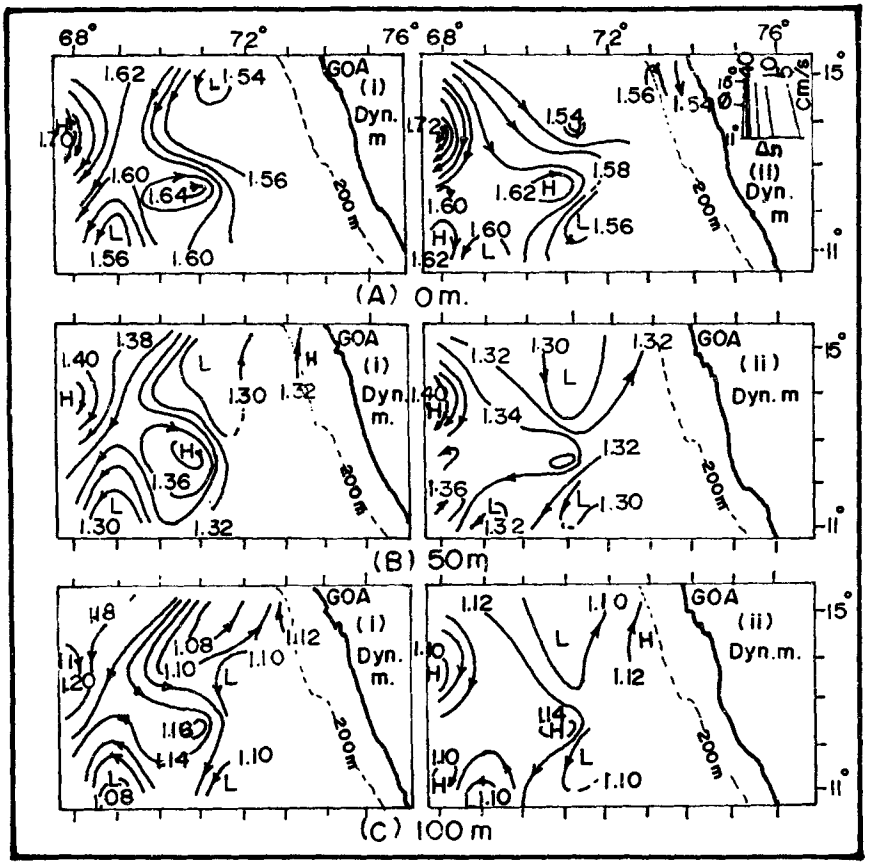

Figure 9. Dynamic topography (meters) of (A) 0 db, (B) 50 db and (C) 100 db surfaces with reference to 1000 db pressure surface during first (i) and second (ii) phases.

fluxes based on the environmental parameters were computed with the help of empirical formulae (Laevastu *et al* 1970) and the conventional bulk aerodynamic expressions. The computations are presented in table 1b. The uncertainties in estimation of fluxes by the bulk aerodynamic expressions are related to the transfer coefficients which depend upon wind speed and stability. However, a constant value ($1{\cdot}4 \times 10^{-3}$) was assigned for the transfer coefficients in view of lower wind speeds ($< 6\,ms^{-1}$) and the lower sea-air temperature difference ($< 2°C$) over the study area (Bunker 1976). The accuracies of fluxes derived from bulk formulae are accordingly limited to about of $\pm 10\%$. We found that the net radiative flux remained more generally steady since the incoming global and effective back radiative fluxes were decreased by the same order of magnitude from May to June. On the other hand, the evaporation and sensible heat fluxes increased by about 20% and 50% respectively in the observational period. This results in a corresponding decrease of the net accumulation of heat at the surface by about 50%. On an average, the net surface heat gain worked out to be $84\,Wm^{-2}$ for both phases.

The average zonal (u) and meridional (v) components of the current for the grid area were estimated and are shown in table 2a. The flow components (u, v) in both

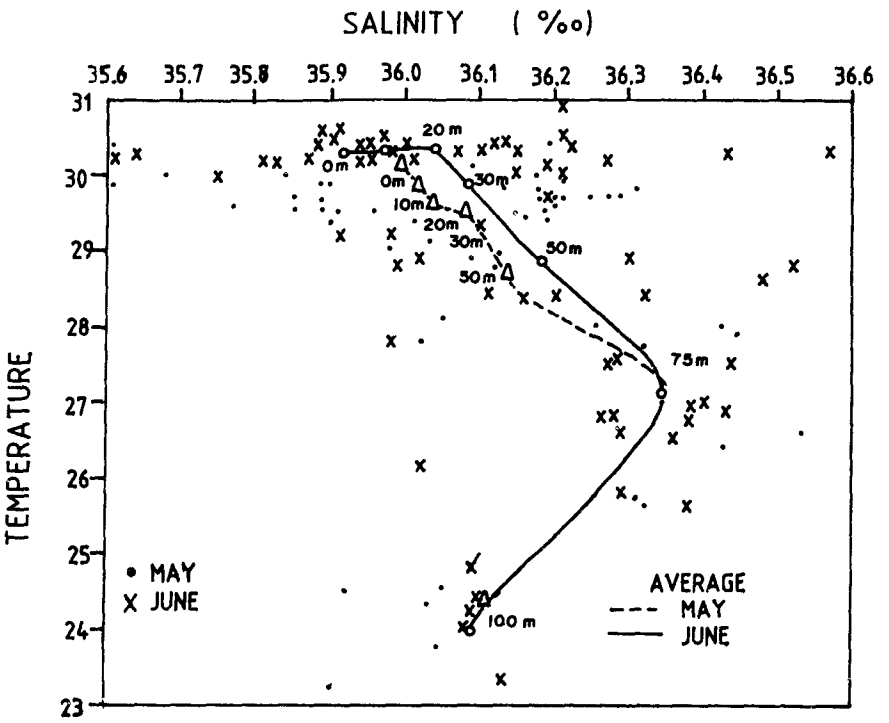

Figure 10. Average T–S profiles in upper 100 m for May and June 1979.

Table 1a. Average surface meteorological parameters for the selected grid region in the study area.

	Phase I	Phase II
Sea surface temperature (°C)	30·0	30·5
Air temperature (°C)	29·0	28·5
Water vapour pressure (mb)	31·7	32·1
Cloudiness (tenths)	—	6·0
Wind speed (ms^{-1})	4·2	5·5

Table 1b. Average surface heat flux (Wm^{-2}) parameters for the selected grid region in the study area.

	Phase I	Phase II	Phases I and II
Global radiation	379	332	356
Effective back radiation	82	42	62
Net radiative flux	297	290	294
Evaporative heat flux	173	206	190
Sensible heat flux	14	26	20
Net surface heat flux	110	58	84

Table 2a. Average heat advection parameters for the selected grid region in the study area.

	Phase I	Phase II	Phases I and II
$\partial H/\partial x$ (calories cm^{-3})	$-3{\cdot}8 \times 10^{-5}$	$-3{\cdot}0 \times 10^{-5}$	$-3{\cdot}4 \times 10^{-5}$
$\partial H/\partial y$ (calories cm^{-3})	$-1{\cdot}6 \times 10^{-5}$	$-0{\cdot}5 \times 10^{-5}$	$-1{\cdot}1 \times 10^{-5}$
u (cm s^{-1})	$-4{\cdot}8$	$-2{\cdot}7$	$-3{\cdot}8$
v (cm s^{-1})	$-5{\cdot}9$	$-9{\cdot}2$	$-7{\cdot}6$
$V{\cdot}\Delta H$ (Wm^{-2})	$-10{\cdot}8$	$-5{\cdot}2$	$-8{\cdot}0$

H: heat content (calories cm^{-2}); u and v: average flow components for upper 100 m.

Table 2b. Premonsoonal heat budget (Wm^{-2}) for the upper ocean (0–100 m) of the selected grid region in the study area.

Net surface heat flux (A)	84
Net advective heat flux (B)	-8
Resultant heat gain (A + B)	76
Observed heat gain	68

the periods were negative, but for a small increase in speed from May to June. The average geostrophic flow for the upper 100 m during the period of study was 8·5 cm^{-1} directed towards the southwest. Based on this value, the net heat advected out of the region was estimated to be around 8 Wm^{-2}. The resultant heat of accumulation by the combined effect of both surface and advective processes was thus 76 Wm^{-2}. This was close to the observed increase in the heat content of about 68 Wm^{-2} within the 15-day period (table 2b). The present study suggests that the net surface heat exchange was the only dominant factor in increasing the temperature of the upper ocean by about 0·5°C during the period studied.

The upward rise of the thermocline in the northwestern region by about 10 m (figure 3d) during June may not be the response to an atmospheric vortex that had swept across the area during the onset of monsoon in 1979. Further, the decrease in the thermocline depth by about 10 m cannot be taken to be a significant one, in view of the uncertainties about the depth of the 20°C isotherm, which represents the thermocline. This is also of the same magnitude as obtained by Swallow *et al* (1983).

The flow patterns maintained a similar picture in May and June over a major part of the area. The only deviation in the flow field from May to June was an onset of southerly baroclinic current across the shelf off Goa, in response to coastal upwelling. This coastal current is due to baroclinic field as a result of sloping steric surfaces with isobaric surfaces. Away from the boundaries, the dominant southerly flow in both phases could influence the development of a strong easterly boundary current south of Sri Lanka (Cutler and Swallow 1984).

The onset of monsoon winds in 1979 took place over the Somali Basin prior to its extension over the eastern Arabian Sea and the adjoining west coast of India. Several studies (Brown *et al* 1980; Düing *et al* 1980; Leetmaa *et al* 1982 and Swallow

et al 1983) have been made on the progressive development of the flow pattern in the Somali basin from April to August 1979. These studies have indicated the onset of a strong Somali boundary current in early May. But remote forcing by the Somali current on the circulation in the east central Arabian Sea was not likely, as the Somali Current turns southwards under the influence of two clockwise gyres that dominate over the western boundary of the Arabian Sea (Düing *et al* 1980; Brown *et al* 1980; and Reverdin and Fieux 1987).

5. Conclusions

The premonsoonal heating in the east central Arabian Sea was controlled by surface heat exchange processes. The contribution by advective heat transfer was only about 10% of the net heat exchange. It was negative as the currents tended to remove heat from the area.

Acknowledgements

The authors thank the late Dr H N Siddique and Dr B N Desai for their keen interest in this study.

References

Bennet E B 1970 *Turbulent diffusion, advection and water structure in the north Indian Ocean.* PhD thesis, University of Hawaii, Hanolulu, Hawaii, pp. 1–133

Brown O B, Bruce J G and Evans R H 1980 Evolution of SST in the Somali Basin during south west monsoon of 1979; *Science* **209** 595–599

Bruce J G 1968 Comparision of near surface dynamic topography during the two monsoons in the western Indian Ocean; *Deep Sea Res.* **15** 655–677

Bunker A 1976 Computation of surface energy flux and annual sea-air interaction cycles of north Atlantic Ocean; *Mon. Weath. Rev.* **104** 1120–1140

Cutler A N and Swallow J C 1984 Surface currents of the Indian Ocean (to 25 S, 100 E): compiled from historical data archived by the Meteorological Office, Bracknell, UK. Institute of Oceanographic Sciences, Report No. 187, 8 pp. and 36 charts

Duing W, Molinari R L and Swallow J C 1980 Somali current: Evolution of surface flow; *Science* **209** 588–589

Krishnamurti T N, Philip A, Ramanathan Y and Richard P 1979 Quick look summer Monex Atlas – part II The onset phase; (Tallahasse: Florida State University), Report No. 79, 205 pp

Krishnamurti T N 1981 Cooling of the Arabian Sea and the onset vortex during 1979; *Recent progress in equatorial oceanography*, SCOR WG Rep No. 47, Venice

Laevastu T, Clarke L and Wolff P M 1970 Annual cycles of heat in the northern hemisphere oceans and heat distribution by ocean currents; (Monterey: Fleet Numerical Weather Central), Tech. Note No. 53, 17 pp

Leetmaa A, Quadfasel D R and Wilson D 1982 Development of the flow field during the onset of the Somali Current, 1979; *J. Phys. Oceanogr.* **12** 1325–1342

Rao R R 1984 A case study on the influence of summer monsoonal vortex on the thermal structure of upper central arabian Sea during the onset phase of Monex 79; *Deep Sea Res.* **12** 1511–1521

Ramesh Babu V and Sastry J S 1984 Summer cooling in the east central Arabian Sea—A process of dynamic response to the south west monsoon; *Mausam* **35** 17–26

Reverdin G and Fieux M 1987 Sections in the western Indian Ocean—Variability in the temperature structure; *Deep Sea Res.* **34** 601–608

Sastry J S and D'Souza R N 1972 Oceanography of the Arabian Sea during southwest monsoon—Part II: Stratification and circulation; *Indian J. Meteor. Geophys.* **22** 33–34

Sharma G S 1968a Thermocline as an indicator of upwelling; *J. Mar. Biol. Assn. India* **8** 8–19

Sharma G S 1968b Seasonal variation of some hydrographical properties of shelf waters off the west coast of India; *Bull. Natn. Inst. Sci. India* **38** 263–276

Sharma G S 1976 Water characteristics and current structure at 65 E during the southwest monsoon; *J. Oceanogr. Soc. Jpn.* **32** 284–296

Sundara Raman K V and Murthy K V S 1968 Geostrophic currents in the eastern Arabian sea during the monsoon season; *Bull. Natn. Inst. Sci. India* **38** 221–235

Sverdrup H U, Johnson M W and Fleming R H 1942 The Oceans: their physics, chemistry and general biology (New York: Prentice-Hall) pp. 1–1087

Swallow J C and Bruce J G 1966 Current measurements off the Somali Coast during the south west monsoon of 1964; *Deep Sea Res.* **13** 861–888

Swallow J C, Molinari R L, Bruce J G, Brown O B and Evans R H 1983 Development of near surface flow pattern and watermass distribution in the Somali Basin in response to the southwest monsoon of 1979; *J. Phys. Oceanogr.* **13** 1398–1415

Varadachari V V R, Murthy C S and Das P K 1968 On the level of least motion and the circulation in the upper layers of the Bay of Bengal; *Bull. Natn. Inst. Sci. India* **38** 301–307

Zaklinskii G B 1964 Deep circulation of waters in the Indian Ocean; *Deep Sea Res.* **11** 286–292